PDGFRα⁺ pericryptal stromal cells are the critical source of Wnts and RSPO3 for murine intestinal stem cells in vivo

Gediminas Greicius[a,1], Zahra Kabiri[a,1,2], Kristmundur Sigmundsson[b], Chao Liang[a], Ralph Bunte[b], Manvendra K. Singh[b], and David M. Virshup[a,c,3]

[a]Program in Cancer and Stem Cell Biology, Duke-NUS Medical School, 169857 Singapore; [b]Program in Cardiovascular and Metabolic Disorders, Duke-NUS Medical School, 169857 Singapore; and [c]Department of Pediatrics, Duke University School of Medicine, Durham, NC 27703

Wnts and R-spondins (RSPOs) support intestinal homeostasis by regulating crypt cell proliferation and differentiation. Ex vivo, Wnts secreted by Paneth cells in organoids can regulate the proliferation and differentiation of *Lgr5*-expressing intestinal stem cells. However, in vivo, Paneth cell and indeed all epithelial Wnt production is completely dispensable, and the cellular source of Wnts and RSPOs that maintain the intestinal stem-cell niche is not known. Here we investigated both the source and the functional role of stromal Wnts and RSPO3 in regulation of intestinal homeostasis. RSPO3 is highly expressed in pericryptal myofibroblasts in the lamina propria and is several orders of magnitude more potent than RSPO1 in stimulating both Wnt/β-catenin signaling and organoid growth. Stromal *Rspo3* ablation ex vivo resulted in markedly decreased organoid growth that was rescued by exogenous RSPO3 protein. *Pdgf receptor alpha* (*PdgfRα*) is known to be expressed in pericryptal myofibroblasts. We therefore evaluated if *PdgfRα* identified the key stromal niche cells. In vivo, *Porcn* excision in *PdgfRα*⁺ cells blocked intestinal crypt formation, demonstrating that Wnt production in the stroma is both necessary and sufficient to support the intestinal stem-cell niche. Mice with *Rspo3* excision in the *PdgfRα*⁺ cells had decreased intestinal crypt Wnt/β-catenin signaling and Paneth cell differentiation and were hypersensitive when stressed with dextran sodium sulfate. The data support a model of the intestinal stem-cell niche regulated by both Wnts and RSPO3 supplied predominantly by stromal pericryptal myofibroblasts marked by *PdgfRα*.

Wnt signaling | stroma | myofibroblasts | intestine | R-spondins

Self-renewal, rapid proliferation, and regulated differentiation are key features of the intestinal stem-cell niche located at the base of the crypts of Lieberkühn, the smallest structural units of the intestinal mucosa (1). The coordinated regulation of these critical events requires tightly controlled activation of the β-catenin signaling pathway by R-spondin and Wnt ligands (2–5). The discovery that intestinal crypts can be propagated in long-term in vitro cultures (6, 7) led to the model that the intestinal stem-cell niche is formed by the close interaction of *Lgr5*⁺ stem cells with adjacent Paneth cells that secrete the necessary Wnt ligands. Consistent with this, ex vivo intestinal stem cells can differentiate into Wnt-producing Paneth cells and so maintain crypts as relatively autonomous units, provided that the environment contains the required growth factors. One of these essential ex vivo growth factors is an R-spondin (RSPO).

The RSPOs are secreted polypeptides that are frequently coexpressed with Wnt genes and are encoded by four paralogous genes, *RSPO1–RSPO4*, found only in vertebrates (8). The function of RSPOs was first uncovered in a screen for Wnt pathway activators in *Xenopus*, where RSPO2 markedly increased sensitivity to Wnt ligands (8). Subsequent studies established that all RSPOs can sensitize cells to Wnts, albeit with varying potency (9–11). While all RSPOs are secreted, the more Wnt-active RSPO2 and RSPO3 are tightly cell-surface associated via bind-

ing to syndecans (12). RSPOs are composed of two furin-like domains, a thrombospondin domain, and a C-terminal basic amino acid-rich domain (13). The second furin domain interacts at the cell membrane with a member of the Lgr4/5/6 family in a heterotrimeric complex, while the first furin domain engages one of two closely related integral membrane ubiquitin ligases, RNF43 or ZNRF3 (14). Formation of this ternary complex prevents RNF43/ZNRF3 from ubiquitylation of the Wnt receptors Frizzled and LRP6, thereby preventing their endocytosis and degradation (15, 16). The net result is enhanced Wnt/β-catenin signaling due to the increased abundance of Wnt receptors on the cell surface (17). Interestingly, while the furin domains of all RSPOs can interact with LGR5, those derived from RSPO2 and RSPO3 have significantly higher affinity than RSPO1 (11). Consistent with this, translocation-induced overexpression of RSPO2 and RSPO3 drives a number of cancers, including human colon and prostate cancers (18–21).

Several studies have examined which R-spondins are required to regulate the stem-cell niche in the normal intestine in vivo. While expressed at very low levels, *Rspo1* is the most highly expressed RSPO in intestinal epithelial cells. Overexpression or parenteral administration of RSPO1 induces a remarkable intestinal hyperplasia, suggesting it could play a functional role in vivo (4, 22). However, as noted, RSPO1 is not a particularly potent

---

Significance

Tissue stem cells in vivo reside in highly structured niches that provide signals for proliferation and differentiation. Understanding the role of the niche requires identifying the key cell types that provide these regulators. In the intestine, R-spondins and Wnts are essential regulators of the stem-cell niche. Here we identify subepithelial myofibroblasts of the PDGF receptor α lineage as the specific stromal cell type that secretes these ligands. These data demonstrate the close interaction between epithelial stem cells and the underlying regulatory stroma niche and provide insights into both normal homeostasis and tissue recovery after injury.

---

regulator of Wnt/β-catenin signaling (9, 10), and intestinal organoids expressing endogenous *Rspo1* and lacking a stromal niche require supplementation with high concentrations (0.5–1 μg/mL) of recombinant RSPO1 to support intestinal organoid growth ex vivo (7). *Rspo2* overexpression in stromal myofibroblasts of the murine colon in response to bacterial infection has been reported in genetically susceptible mouse strains (although not in BL/6 mice), but *Rspo2* was not detectable under nonstressed conditions (23, 24). *Rspo3* is the most highly expressed RSPO in the intestine (24). Supporting a role for *Rspo3*, inhibition of RSPO3 with a neutralizing antibody caused a decrease in *Lgr5* expression (5). Combined neutralization of RSPO2 and RSPO3 produced more substantial inhibition of *Lgr5* expression and delayed crypt regeneration only after stress (5). The nature of the cells that produce the functionally important RSPOs is unknown. We reported that intestinal organoids, when cocultured with intestinal stroma from nonstressed mice, can be grown in the absence of added RSPO1, suggesting the stroma itself could be the major source of an RSPO in vivo as well (24).

Here, we address the source and functional role of RSPO3 as a component of the intestinal epithelial stem-cell niche. Our studies indicate that subepithelial myofibroblasts marked by *PdgfRα* expression are an essential source of Wnts as well as a critical source of RSPO3.

Results

RSPO3 as a Cytokine-Like Enhancer of the Wnt/β-Catenin Signaling Pathway. While RSPO1 is generally regarded as a key regulator of Wnt signaling in the intestinal crypt, we previously found that *Rspo3* is by far the most abundant R-spondin expressed in intestinal stromal cells (24). We therefore compared the activity of RSPO3 with the second most abundant RSPO, RSPO1, in WNT/β-catenin reporter assays using purified proteins. The WNT3A-expressing cell line STF3A with an integrated luciferase-based β-catenin reporter SuperTopFlash (STF) (25) was stimulated with increasing concentrations of recombinant RSPO1 or RSPO3. As shown in Fig. 1C, while both factors markedly stimulated Wnt/β-catenin signaling, RSPO3 was ~200-fold more potent than RSPO1. The EC$_{50}$s were 0.36 and 70.8 ng/mL, respectively, corresponding to ~10 pM RSPO3. As an independent test of the relative activities of RSPO1 and RSPO3, we repeated the reporter assays using expression plasmids encoding tagged versions of RSPO1 and RSPO3. As shown in Fig. 1 *A* and *B*, while the plasmids directed the expression of roughly equal amounts of protein, transiently expressed RSPO3 was a significantly more potent enhancer of Wnt/β-catenin than RSPO1 at all plasmid concentrations tested. Taken together, the data confirm that RSPO3 is significantly more potent than RSPO1 in enhancing Wnt/β-catenin activation. Moreover, the biologically active concentrations of RSPO3 are in the picomolar range, resembling those of biologically active cytokines.

RSPO3 Supports Intestinal Organoid Growth in Vitro. Having established that RSPO3 is more potent than RSPO1 in HEK293 cells, we next compared the ability of RSPO1 and RSPO3 to support Wnt-dependent epithelial stem-cell proliferation and differentiation in vitro. Gut epithelial crypt preparations were incubated with the indicated concentrations of RSPO1 or RSPO3 for 5 d and then scored for organoid formation as well as expression of stem-cell and lineage-differentiation markers (Fig. 1 *D–F*). At saturating concentrations RSPO1 and RSPO3 supported organoid growth equally well. However, at limiting concentrations RSPO3 was significantly more potent than RSPO1 in its ability to support growth of intestinal organoids, with an EC$_{50}$ at 6.4 ng/mL versus 74.4 ng/mL (Fig. 1D). RSPO3 was also significantly more active than RSPO1 at increasing the expression of Wnt/β-catenin target and intestinal stem-cell genes and at suppressing the expression of the goblet cell-specific gene *Muc2* (Fig. 1F). Taken together, the data indicate that RSPO3 is significantly more po-

Fig. 1. RSPO3 is more potent than RSPO1 in activating a β-catenin reporter and supporting intestinal organoid cultures. (*A*) STF3A cells were transfected with the indicated amounts of RSPO1 and RSPO3 expression plasmids, and the resultant Wnt/β-catenin–dependent luciferase signal was measured as described. (*B*) Comparative RSPO1-Myc and RSPO3-Myc expression levels in transfected STF3A cells assessed by anti-MYC immunoblot. Mw, molecular weight. (*C*) Recombinant RSPO3 and RSPO1 were added at the indicated concentrations to HEK293 STF3A cells with robust endogenous Wnt signaling as described. Data from two independent experiments with similar results were normalized and merged, with the activity induced by 200 ng/mL RSPO1 set as 100%. (*D*) RSPO3 is more potent than RSPO1 in promoting organoid growth. Organoids were cultured with the indicated concentration of RSPO and counted in three wells per group on day 5. Data from two independent experiments were equalized using the organoid count in the RSPO1 500 ng/mL group as 100% response. (*E*) RSPO1- and RSPO3-stimulated organoids have similar morphologic features. Organoids were cultured in the presence of the indicated R-spondin concentrations and photographed on day 5. (Scale bar: 100 μm.) (*F*) RSPO3 is more potent than RSPO1 in regulating differentiation in intestinal epithelial organoids. The expression of the indicated differentiation markers from the organoids in *D* was assessed at day 5, normalized to β-actin expression levels. The figures combine two independent experiments, equalized by setting the expression in the RSPO3 100 ng/mL group as 100% response. *$P < 0.05$, Wilcoxon rank sum test.

tent than RSPO1 in maintaining crypt-derived intestinal stem cells and may be sufficient to potentiate Wnt signaling in the maintenance of intestinal homeostasis.

RSPO3 Is Expressed in Pericryptal Intestinal Myofibroblasts. We examined if RSPO3 expression was anatomically positioned to regulate the intestinal stem-cell niche. RSPO3 protein was present in pericryptal cells in the mouse intestine as assessed by indirect immunofluorescence microscopy (Fig. 2A), consistent with

the abundant expression of *Rspo3* mRNA in intestinal myofibroblasts (24). To better characterize the specific cells expressing *Rspo3*, intestinal myofibroblasts were purified as previously described (24); the coexpression of stromal markers was assessed by indirect immunofluorescence microscopy, and expression was machine-scored using high-content screening algorithms (Fig. 2B). RSPO3 was coexpressed with smooth muscle actin (SMA) and was generally not present in desmin-positive and FSP-1–positive cells, consistent with its expression in pericryptal myofibroblasts (26–28).

To verify the specificity of the RSPO3 antibody, we obtained C57BL/6 mice with a floxed allele of *Rspo3* that were generated by John Cobb at the University of Calgary, Calgary AB, Canada (29). Freshly cultured *Rspo3*^fl/fl small intestinal stromal cells, predominantly consisting of myofibroblasts, were infected with Cre/GFP- or control GFP-expressing adenoviruses. Based on GFP expression, we estimate that infection efficiency was consistently at least 70–80%, and the cellular viability was not affected by the expression of *Cre*. *Rspo3* excision led to the loss of RSPO3 immunoreactivity, demonstrating both efficient gene excision and the specificity of the antibody (Fig. S1A). As an additional test of specificity, the immunostaining of intestinal pericryptal cells by the RSPO3 antibody was blocked by inclusion of the RSPO3 antigenic peptide (Fig. S1B), and immunostaining was also lost in an *Rspo3* knockout, as described below (Fig. S1C).

Stromal Rspo3 Is Necessary for the ex Vivo Stem-Cell Niche. Intestinal epithelial cells are dependent on niche-produced Wnts, enhanced by R-spondins, to maintain intestinal homeostasis. *Rspo3* is the most highly expressed RSPO in the stroma, but because it encodes a diffusible factor, whether its expression in myofibroblasts is

necessary to support crypt proliferation is not established. We previously used coculture of wild-type stroma with *Porcn*-knockout intestinal epithelium to demonstrate that stromal cells could replace both the need for exogenous RSPO1 and epithelial Wnt production (24). Here we investigated if stromal Wnts and RSPO3 are necessary for the growth of *Porcn*-deficient organoids. To achieve this, we modified the stroma coculture system to allow in vitro gene knockout or knockdown using Cre-expressing adenoviruses or siRNA, respectively. As shown in Fig. S2, *Porcn*^−/− epithelial cells require *Porcn*-expressing stroma to form organoids. Adenoviral-mediated expression of Cre in the *Porcn*^fl/fl stromal cells gave *Porcn*^−/− stroma that could no longer support organoid growth. This result confirmed both that we could achieve gene targeting and that stroma-produced Wnts are essential for epithelial cell proliferation in this system.

We examined if stromal *Rspo3* expression was necessary and sufficient in the ex vivo crypt plus stroma organoid assay (Fig. 3B). Confirming that stromal cells are a robust source of RSPOs, supplementation with recombinant RSPO3 had no effect on organoid counts in the control wells. However, knockdown of *Rspo3* in stromal cells by siRNA before coculture with *Porcn*^−/− epithelial cells reduced the organoid counts 30–50%. Importantly, the decrease in organoids was not due to an off-target effect of siRNA, as it could be rescued by supplementation with recombinant RSPO3 protein. As a second approach, we excised *Rspo3* ex vivo. Intestinal stromal cells derived from mice carrying homozygous floxed *Rspo3* alleles were infected with adenovirus expressing Cre/GFP (targeting) or GFP alone (mock targeting). *Rspo3*-excised stroma was markedly deficient in supporting organoid formation (Fig. 3B, *Lower*). Confirming that this defect is due to the loss of *Rspo3* expression, organoid counts were restored to control numbers in the presence of recombinant RSPO3. Taken together, our findings demonstrate that RSPO3 production from intestinal stromal cells is necessary and is not compensated by RSPO1 and RSPO2 for intestinal epithelial stem-cell proliferation and differentiation in this ex vivo model.

PdgfRα-Cre⁺ Marks Rspo3-Expressing Intestinal Stromal Cells. To knock out stromal Wnt and RSPO3 production in vivo, we examined the literature for genetic markers expressed in subepithelial myofibroblasts. *PdgfRα* stood out as a candidate, as *PdgfRα*^+ stromal cells are required for early intestinal morphogenesis, including the formation of intestinal villi, and stromal cells immediately adjacent to crypt and villus basement membrane express PGDF receptor alpha (PDGFRα) (30, 31). We examined the expression of *PdgfRα–Cre* in the guts of transgenic mice (32) by crossing them with *Rosa*^mTmG reporter mice (33). In the resulting crosses, the *PdgfRα*-expressing cells undergo Cremediated recombination to silence membrane-targeted Tomato red fluorescent protein (mT) and express instead a membrane-targeted GFP. As shown in Fig. 4A and Fig. S4, *PdgfRα*-lineage⁺ (GFP⁺) cells form a single layer of cells directly apposed to the basement membrane adjacent to the basal surface of the intestinal epithelial cells, a position that is consistent with the known localization of subepithelial myofibroblasts and telocytes (31). In contrast to RSPO3 immunostaining that was enriched at the base of the crypts, the *PdgfRα-Cre* GFP-labeled cells outlined all subepithelial basal surfaces (Fig. S4), suggesting that RSPO3-expressing cells are a subset of the *PdgfRα*-lineage cells. To address whether *PdgfRα-Cre*–lineage cells also expressed *Rspo3*, we cultured intestinal stromal cells from *PdgfRα-Cre*⁺/*Rosa*^mTmG mice, sorted them into *PdgfRα*⁺ (GFP⁺) and *PdgfRα*⁻ (mTomato⁺) populations using flow cytometry, and then assessed their *Rspo3* levels using qPCR. Approximately two-thirds of the cultured stromal cells were GFP⁺. The GFP⁺ (*PdgfRα*-lineage) stromal cells were a rich source of *Rspo3*, expressing ~15-fold more than did the *PdgfRα*⁻ stromal cells

Fig. 2. The majority of RSPO3-expressing cells are pericryptal myofibroblasts. (*A*) Frozen sections of normal mouse colon or small intestine as indicated were labeled with antibodies specific for RSPO3 (red) and E-cadherin (green) or with nonspecific primary IgGs from the respective species; nuclei were counterstained with Hoechst. Pericryptal cells positive for RSPO3 are indicated with white arrows. (Scale bars: 50 μm.) (*B, Upper*) RSPO3 is coexpressed with SMA. Purified stromal cells were cultured for 7 d, fixed, and costained with antibodies specific for RSPO3 (yellow) and the myofibroblast-specific marker SMA (red), as well as desmin (red) and fibroblast-specific protein 1 (FSP1) (red), as indicated. (Scale bars: 90 μm.) (*Lower*) Quantitation of costaining using Columbus software. At least 450 cells were quantified per group. The percentage of cells in each quadrant is indicated. The quantification was repeated three times with similar results.

A Co-culture in the absence of external RSPO3

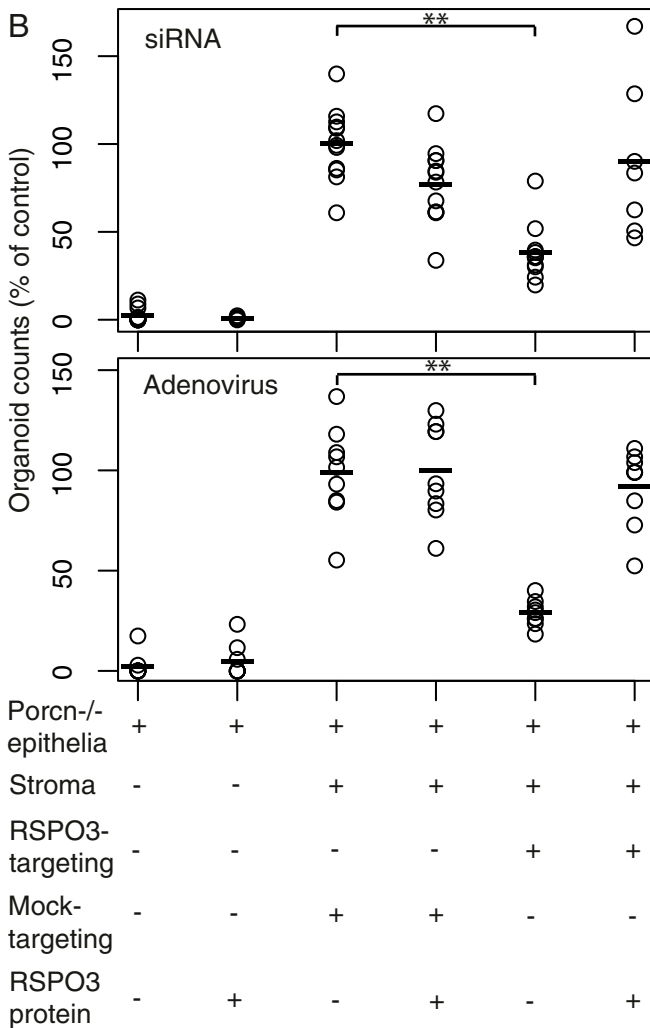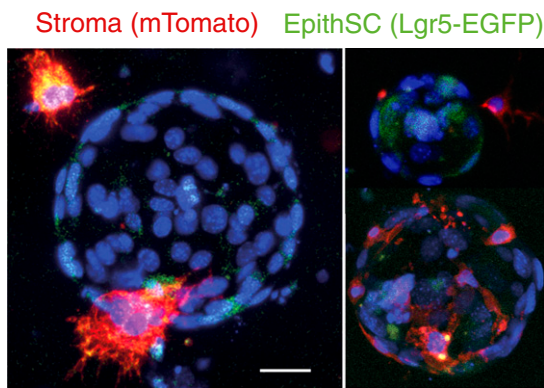Stroma (mTomato) EpithSC (Lgr5-EGFP)

Fig. 3. Stromal RSPO3 and Wnts are critical for adult intestinal homeostasis. (A) Intestinal stromal cells contact Lgr5-expressing cells in vitro. mTomato-expressing stromal cells from *Rosa^mTmG* mice were combined with purified epithelial crypts from *Lgr5-GFP* mice. The mixed cells were cultured without added RSPO for 5 d and then were imaged using an inverted Zeiss LSM 710 microscope. Intestinal stroma, Lgr5⁺ cells, and nuclei are labeled red, green, and blue, respectively. (Scale bar: 20 μm.) (B) Stromal RSPO3 is required for organoid growth. PORCN-deficient intestinal epithelial cells requiring Wnts from stroma were cultured either alone or in combination with intestinal stromal cells. *Rspo3* expression was targeted using siRNA (*Upper*) or adenoviral-expressed Cre (*Lower*). Mock targeting was performed with scrambled siRNA or

(Fig. 4B). To visualize the interaction of the *Rspo3*⁺ stromal cells with organoids, we cultured a mix of GFP⁺ and mTomato⁺ stromal cells from *PdgfRα-Cre*⁺/*Rosa^mTmG* mice with crypts from *Porcn*-deficient mice. As before, this stroma rescues the growth of *Porcn*-null organoids. The rescued organoids were imaged after 4 d of culture, at a time when crypts cultured in the absence of myofibroblasts had failed to grow. Virtually all the rescued organoids had *PdgfRα*⁺/*GFP*-expressing stromal cells in close proximity, often with long cellular extensions appearing to contact the epithelial cells (Fig. 4C). We conclude that the *PdgfRα* promoter is active in the subepithelial myofibroblast lineage and that *Rspo3*⁺ *PdfgRα*⁺ subepithelial myofibroblasts have the characteristics of stromal niche cells.

PORCN from *PdgfRα*-Lineage Cells Is Required for Neonatal Crypt Formation. We considered what phenotype would be caused by loss of Wnt and RSPO production from intestinal stromal cells. During embryonic intestinal development, epithelial villi are formed independent of canonical Wnt signaling, as neonatal mice either lacking TCF4 or expressing the Wnt inhibitor DKK1 in the gut have normal villus architecture but lack normal crypts (3, 34). While intestinal stem cells are found at birth, they are located in the epithelium between villi. These intestinal stem cells are identified by Wnt-dependent proliferation that leads to the formation of intervillous crypts a few days after birth (35, 36). Hence, we expected that an intestinal Wnt phenotype should be present only after birth.

To ablate Wnt secretion in stromal myofibroblasts, we crossed *PdgfRα-Cre* mice with *Porcn^fl/fl* mice. Mice with targeted excision of *Porcn* were grossly indistinguishable from their littermates at birth, but ∼50% died by day 6. For analysis of intestinal development, pups were killed on postnatal day 5. The pups were able to feed, as judged by the presence of milk in the stomach. *PdgfRα-Cre*⁺/*Porcn^fl/fl* pups had normal embryonic intestinal development, as demonstrated by the presence of villi (3). However, the intestines from *PdgfRα-Cre*⁺/*Porcn^fl/fl* pups had markedly fewer intestinal crypts and significantly fewer proliferating cells, as assessed by 5-ethynyl-2′-deoxyuridine (EdU) incorporation (Fig. 5A). Consistent with decreased Wnt/β-catenin signaling, we detected decreased levels of the Wnt target gene *Axin2* (Fig. 5 A and B). Interestingly, *Porcn*-excised mice also had decreased proliferation in the lamina propria, consistent with reports of β-catenin activity in intestinal stroma (Fig. 5C) (37). Our findings demonstrate that *PdgfRα*-lineage intestinal stromal cells are a critical source of Wnts during postnatal intestinal morphogenesis.

RSPO3 Derived from Myofibroblasts Is Not Essential for Normal Intestinal Homeostasis. Having found that PdgfRα⁺-lineage stromal cells are key regulators of Wnt signaling in early intestinal morphogenesis, we next used the same Cre driver to ablate *Rspo3* expression. Consistent with the expression of *PdgfRα-Cre* in a subset of stromal cells, we detected successful but partial excision of the floxed *Rspo3* exon in intestinal DNA (Fig. S3). Excision of *Rspo3* in *PdgfRα*-lineage myofibroblasts also caused a significant but partial decrease in *Rspo3* expression in both ileum and colon (Fig. 6A). To test the efficacy of excision specifically in the *PdgfRα*-lineage myofibroblasts, GFP⁺ cells were isolated from *PdgfRα-Cre*/*Rosa^mTmG*/*Rspo3^fl/fl* intestinal stroma, and gene expression was compared with mTomato⁺/GFP⁻ cells. *Rspo3* expression was entirely ablated in the targeted cells. The GFP⁺ cells specifically expressed the myofibroblast marker *Acta2*/SMA

GFP-expressing adenovirus, respectively. In the rescue, RSPO3 (50 ng/mL) was added. Combined data from four siRNA and three viral-targeting experiments are presented. **P < 0.001, Wilcoxon rank sum test.
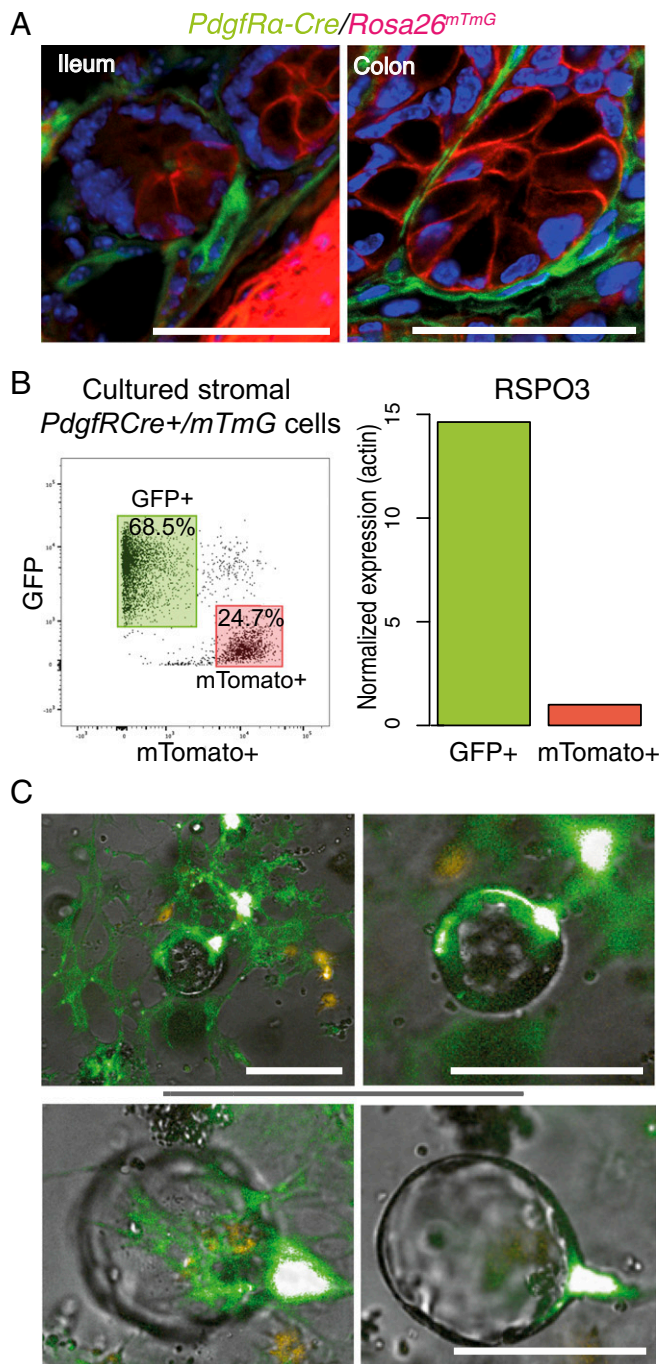
A *PdgfRα-Cre/Rosa26^mTmG*

Ileum | Colon

B Cultured stromal *PdgfRCre+/mTmG* cells

RSPO3

GFP+ 68.5%

mTomato+ 24.7%

C

Fig. 4. *PdgfRα-Cre*–driven GFP reporter activation labels pericryptal myofibroblasts. (*A*) Samples from ileum and colon of *PdgfRα-Cre^+^/Rosa^mTmG^* mice were fixed, prepared, and stained with GFP-specific antibodies as described in *Methods*. Nuclei were stained with DAPI. The image is representative of the intestinal crypts of the three mice analyzed. (Scale bars: 50 μm.) (*B*) *PdgfRα-Cre*–labeled cells express RSPO3. *PdgfRα-Cre^+^/Rosa^mTmG^* myofibroblasts were prepared, cultured for 10 d, and FACS-sorted into GFP^+^ and mTomato^+^ populations. (*Left*) The proportion of positive cells in the population is presented as a percentage in a respective gate. (*Right*) *Rspo3* expression levels were analyzed by qRT-PCR and normalized to *Actb*. (*C*) *PdgfRα-Cre*–labeled cells support *Porcn*-deficient organoids. *PdgfRα-Cre^+^/Rosa^mTmG^* myofibroblasts were prepared, cultured for 10 d, and mixed with *Porcn*-deficient epithelial cells. The mixed cell cultures were incubated for 4 d and photographed thereafter. Images of two organoids at different focal planes are representative of two experiments with similar results. (Scale bars: 100 μm.)

as well as *Gli1*. In addition, they had enriched but not exclusive expression of *FoxL1*, *Grem2*, and *Myh11* (Fig. S5).

The effects of stromal *Rspo3* excision were more subtle than seen with *Porcn* excision. *PdgfRα-Cre^+^* mice heterozygous and homozygous for the *Rspo3^fl^* allele were phenotypically indistinguishable from wild-type littermates. Intestinal morphology appeared normal in weaned mice, and there were no significant changes in proliferation in the crypts (Fig. 6*B*). However, consistent with a modest decrease in Wnt signaling after homozygous stromal *Rspo3* excision, the expression of the Wnt target genes *Axin2* and *Lgr5* was decreased ~30% (Fig. 6*C*), and there was a decrease in Paneth cell differentiation, a Wnt-driven process (38), as assessed by both lysozyme protein (Fig. 6*B*) and mRNA (Fig. 6*C*) expression. This phenotype resembles that seen in mice administered an anti-RSPO3 neutralizing antibody (5), indicating that *PdgfRα*-lineage cells are a functionally important source of RSPO3 in the mouse intestine.

Rspo3 Ablation in PdgfRα-Expressing Cells Predisposes to Dextran Sodium Sulfate-Induced Colitis. Intrigued by the observation that down-regulation of Wnt target genes in *PdgfRα-Cre^+^/Rspo3^fl/fl^* mice does not markedly perturb normal intestinal homeostasis, we challenged these mice with dextran sulfate sodium (DSS), a treatment that induces colitis and increased intestinal regeneration. Twelve-week-old mice received 2.5% DSS in drinking water ad libitum over the course of 5 d. As shown in Fig. 7*A*, mice with stromal *Rspo3* excision lost weight more rapidly during treatment and at day 5 had a significantly shorter colon length, two findings indicative of a more substantial inflammatory response. Histological analysis of colons from DSS-treated mice revealed that mice with stromal *Rspo3* excision had effacement of normal epithelial architecture and loss of crypts (Fig. 7 *B* and *C*). Thus, we conclude that RSPO3 protein produced by *PdgfRα*-lineage stromal myofibroblasts modulates Wnt signaling in nonstressed conditions and is required to repair epithelial damage caused by DSS-induced colitis.

Discussion

Wnts and R-spondins cooperate to maintain homeostasis in the intestinal crypts. Multiple studies have suggested that in vivo Wnts and RSPOs from the stromal compartment are required for intestinal homeostasis. To fully understand the regulation of this signaling, it is essential to identify the stromal cells that supply these ligands to the intestinal stem cells. The stroma of the gut consists of multiple cell types including fibroblasts, myofibroblasts, fibrocytes, hematopoietic cells, and neural and enteric glial cells (28). While highly specific markers for these cellular populations are not well defined, cells expressing *Foxl1* and *Gremlin1* have been shown to express *Wnt2b*, *Wnt5a*, *Rspo1*, and *Rspo3* and to regulate the intestinal stem-cell niche (39). Similarly, pericryptal *Rspo1*-expressing CD34^+^ cells have been shown to modulate the response to DSS-induced colitis (40). These studies provide important insights into the pericryptal stromal cell populations but do not clarify which population is essential for Wnt and RSPO production. Here we show that intestinal subepithelial myofibroblasts marked by the expression of *PdgfRα* are an essential source of both Wnts and RSPO3 in the mouse intestine.

Extensive data indicate PDGFRα is important in the intestinal stroma. While *PdgfRβ* is involved in vascular development, *PdgfRα*-expressing cells are found in the mesenchyme of lung, gut, and kidney as well as in glial and adipocyte precursors (32, 41–43). In the gut a subset of lamina propria and tunica muscularis cells is labeled in the *PdgfRα-Cre^+^/Rosa^mTmG^* mouse. PDGFRα and its ligand PDGF-A play an important functional role in villus morphogenesis and regeneration (30). PDGFRα was localized by immunostaining to the pericryptal compartment
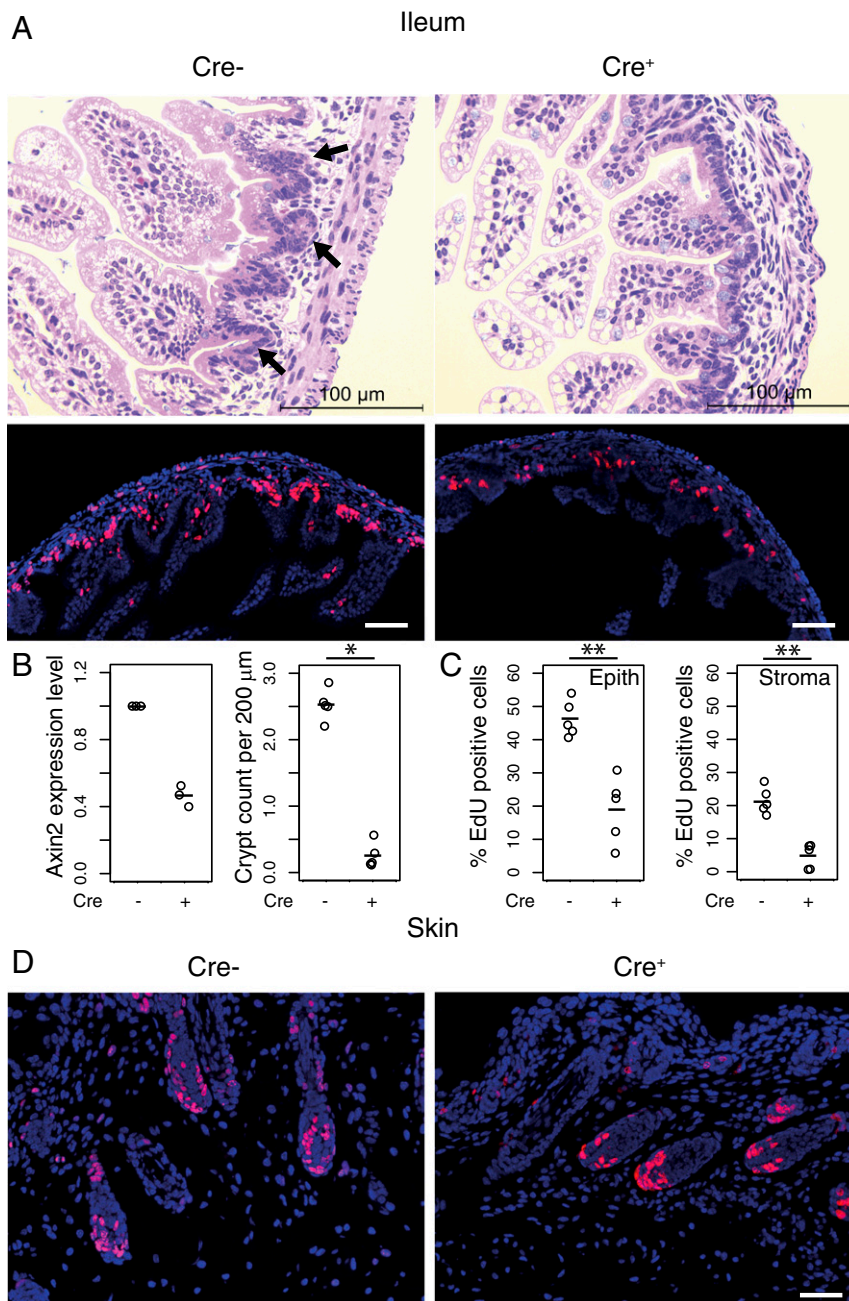
Fig. 5. *Porcn* ablation in *PdgfRα*-expressing cells inhibits crypt formation in the neonatal gut. Intestines from *PdgfRα-Cre⁺/Porcn^fl/fl* mice were harvested on postnatal day 5 and processed as described in *Methods*. (*A*) Intestinal (*Upper*) and abdominal skin (*Lower*) tissues were subjected to H&E or EdU staining, respectively. The figure represents one pair of littermates representative of six littermates analyzed. Arrows indicate newly formed crypts. (Scale bars: 100 μm.) (*B*) *Porcn* excision in *PdgfRα-Cre*–lineage cells leads to decreased *Axin2* expression levels (*Left*) and decreased crypt counts (*Right*). Crypts were counted using histological sections from five littermates in each group. (*C*) *Porcn* excision in *PdgfRα-Cre*–expressing cells leads to significantly decreased numbers of proliferating cells in the epithelial layer of lamina propria and stroma. Proliferating cells were counted in either the top layer of mucosa, which typically represents epithelia, or deeper stromal layers in samples from five littermates and are presented as a ratio to total Hoechst 33342-labeled nuclei. (*D*) *Porcn* excision in *PdgfRα-Cre* mice does not inhibit proliferation in bulbs of skin hair follicles. Images are representative of samples of abdominal skin of three littermates per group that were analyzed. (Scale bar: 100 μm.) *$P < 0.05$, **$P < 0.01$, Wilcoxon rank sum test.

in adult intestinal lamina propria (44). Hence, *PdgfRα* is well positioned to be a marker for stromal niche cells.

PDGFα and CD34 are also expressed in a subpopulation of stromal cells referred to as "telocytes" (31). Telocytes are named for their characteristic long cytoplasmic extensions and were suggested to have a role in cell-to-cell communication (45). However, the nature of this putative communication has not been addressed so far. If the Wnt-expressing cells are indeed telocytes,

we speculate that the defining projections from these cells may also extend across the basement membrane to contact the Wnt-responsive epithelial cells in the crypts, similar to the filopodia transporting Wnts that have been visualized in zebrafish (46).

Wnts and R-spondins are required for the ex vivo proliferation of intestinal epithelial organoids (6, 7, 47). However, how the ex vivo culture relates to in vivo growth is not fully understood. Two competing models describe the relationship between organoids
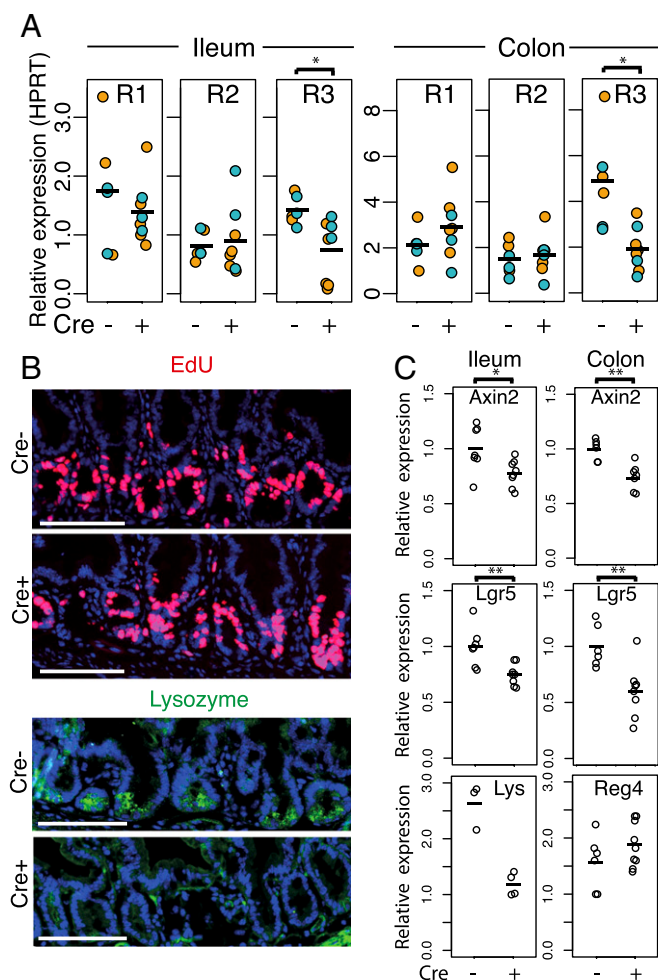
Fig. 6. RSPO3 excision in intestinal myofibroblasts does not perturb normal intestinal homeostasis. (*A*) *PdgfRα-Cre$^+$/Rspo3$^{fl/fl}$* mice express significantly less *Rspo3*. Samples from ileum (*Left*) and colon (*Right*) of male (turquoise) and female (orange) *PdgfRα-Cre$^+$/Rspo3$^{fl/fl}$* and *PdgfRα-Cre$^-$/Rspo3$^{fl/fl}$* mice were collected and analyzed for RNA expression. All samples were normalized to HPRT and then normalized. Mean Ct values of 28.4–30.4, 30.6–31.6, and 26.9–27.4- were obtained for *Rspo1*, *Rspo2*, and *Rspo3*, respectively, in the *Rspo3* nonexcised group. (*B*) *PdgfRα-Cre$^+$/Rspo3$^{fl/fl}$* mice have a decrease in lysozyme-producing Paneth cells but no decrease in intestinal crypt proliferation. Samples from EdU-pulsed *PdgfRα-Cre$^+$/Rspo3$^{fl/fl}$* and *PdgfRα-Cre$^-$/ Rspo3$^{fl/fl}$* mice were prepared and stained with EdU- and lysozyme-specific reagents. Pictures are representative of two mice analyzed from each group. (Scale bars: 100 μm.) (*C*) *Rspo3* excision in *PdgfRα-Cre*–lineage cells leads to decreased abundance of *Axin2*, *Lgr5*, and lysozyme (*Lys*) mRNA in full-thickness slices. Expression levels were normalized to *Hprt*. *$P < 0.05$, **$P < 0.01$, Wilcoxon rank sum test.

and in vivo crypt proliferation. One model, based on results from in vitro systems supplemented with high concentrations of RSPO1, suggests that Paneth cells can provide all necessary Wnts required to maintain Lgr5 cells and sustained proliferation. The in vivo relevance of this model is challenged by results from mice that are deficient in Paneth cells (48, 49), Wnt3 (50), or global epithelial Wnt secretion following *villin-Cre*–driven deletion of *Porcn* and *Wls* (24, 51). All these mice have normal intestinal homeostasis. Thus, an alternative model gaining currency holds that epithelial Wnts are not involved in in vivo stem-cell maintenance and that intestinal stromal cells form the stem-cell niche by producing the necessary Wnts and R-spondins. The key test of this model is to abrogate PORCN and RSPO expression from specific stromal cells. San Roman et al. (51) found

no intestinal defect in tamoxifen-treated *PorcnFl/Y;Myh11-CreERT2* mice, and, similarly, we found no gut phenotype in tamoxifen-treated *Rosa26CreERT2/Porcn$^{fl/fl}$* mice (52). On the surface, these results are in conflict with the current study using a constitutive *Pdgfrα*-CRE. However, we have observed that the PDGFRα$^+$ intestinal stroma is relatively resistant to tamoxifen, for reasons we are actively exploring. The failure of the neonatal gut to form crypts in the setting of constitutive stromal *Porcn* deletion strongly supports the second model, where stromal rather than epithelial Wnt production is of critical importance.

A second finding is that RSPO3 is a key in vivo R-spondin and that it is also produced in the *PdgfRα$^+$*-lineage intestinal stromal cells. RSPO3 is far and away the most abundant R-spondin expressed in the mouse small intestine, and it is produced almost exclusively in the stroma (24). Consistent with our findings
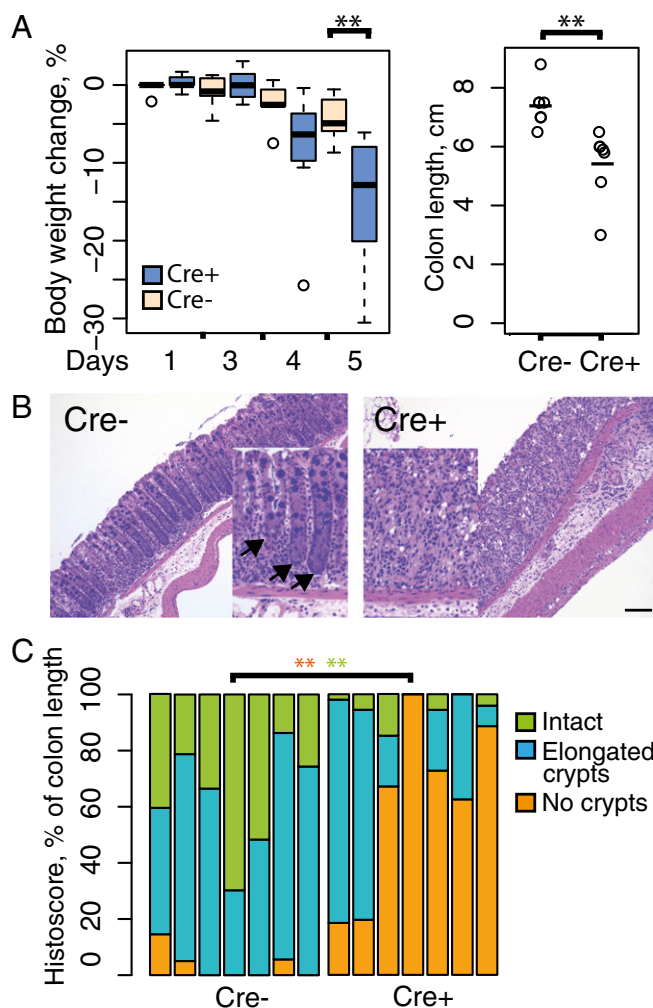

Fig. 7. *Rspo3* excision in intestinal myofibroblasts predisposes to DSS-induced colitis. (*A*, *Left*) *PdgfRα-Cre$^+$/Rspo3$^{fl/fl}$* mice treated with DSS for 5 d rapidly lose weight. **$P = 0.007$, Wilcoxon rank sum test. (*Right*) Colon length was significantly shorter in knockout mice at the end of 5 d treatment. **$P = 0.002$, Wilcoxon rank sum test. (*B*) *PdgfRα-Cre$^+$/Rspo3$^{fl/fl}$* mice display extensive inflammatory infiltrates in the lamina propria and inflammation-associated crypt loss after 5 d of DSS treatment (*Right*) compared with nontargeted controls (*Left*). (*C*) Quantification of inflammation-affected regions after 5 d of DSS treatment. *Rspo3*-deleted (labeled as Cre+) intestines indicate significantly higher crypt loss compared with *Rspo3$^{fl/fl}$* or *PdgfRα-Cre$^+$/Rspo3^{wt}* controls (labeled as Cre–). **$P = 0.0019$ and $P = 0.0032$ for areas with no crypts and those with intact crypt morphology, respectively, Wilcoxon rank sum test.

DEVELOPMENTAL BIOLOGY

on the importance of *Rspo3* in the gut, de Sauvage and co-workers (5) demonstrated that mice treated with RSPO3-neutralizing antibodies had reduced *Lgr5* expression but were otherwise normal. In their study, the addition of an RSPO2-neutralizing antibody further reduced *Lgr5* expression but still did not alter gut morphology. A related study also did not report gut toxicity following RSPO2 or RSPO3 inhibition in unstressed mice (21). A more profound global inhibition of RSPO signaling by systemic overexpression of soluble RSPO receptors resulted in complete degeneration of intestinal crypts (4), suggesting that very small amounts of RSPOs, perhaps systemically supplied, are sufficient to maintain the gut in the absence of stress. However, during intestinal stress induced by either ionizing radiation (5) or DSS (this study), the R-spondin–deficient mice fail to respond adequately. The finding that specific deletion of *Rspo3* in *PdgfRα+* stromal cells produces a phenotype similar to both systemic RSPO3 inhibition and intestinal *Lgr4* knockout (53) demonstrates the critical role of the pericryptal myofibroblasts as the stem-cell niche in the response to injury. Taken together with our previous finding that stromal Wnt production is sufficient to support intestinal homeostasis (24), our current studies support a model in which the intestinal stem-cell niche is regulated by Wnts and RSPO3 supplied by pericryptal myofibroblasts.

Materials and Methods

Mice. *Porcn^fl^* mice (54) were backcrossed to C57BL/6 mice for at least 10 generations. To generate *Porcn*-deficient intestinal epithelial cells, *Porcn^fl^* mice were crossed with BL/6 *Villin-Cre* mice as previously described (24). *Lgr5-EGFP-IRES-CreER^T2^* (55), *Gt (ROSA)26Sor^tm4 (ACTB-tdTomato,-EGFP)Luo^* (33) (referred to as "*Rosa^mTmG^*"), and C57BL/6-Tg(Pdgfra-cre)1ClcI/J (referred to as "*PdgfRα-Cre*") mice were obtained from Jackson Laboratories. All mouse procedures were approved by the Singapore Health Services (SingHealth) Institutional Animal Care and Use Committee.

Organoid Cultures and siRNA Transfection. Crypt and stroma isolation and culture were performed as previously described (24, 55). An *Rspo3*-specific siRNA pool and a pool of scrambled siRNAs were purchased from Santa Cruz Biotechnologies (catalog nos. sc-152619 and sc-37007, respectively) and diluted according to the manufacturer's recommendations. Stromal cells were cultured to 95% confluency and then transfected with siRNA using RNAiMax at the ratio 1 μL:1.5 μL of RNAiMAX (Life Technologies) in RPMI 1640 supplemented with 10% FCS and 1% antibiotics. For coculture assays cells were harvested 48 h after siRNA transfection and used according to the coculture procedures described above.

Adenoviral Infections. Adenoviruses were obtained from Vector Biolabs. We found that optimal infection and viability were obtained using adenoviral mixtures prepared by combining adenovirus expressing Cre/GFP or GFP alone [at a multiplicity of infection (MOI) of 3.25] with AdenoNull adenovirus (Adeno CMV Null, Vector Biolabs, at an MOI of 30). Intestinal stromal cells prepared as described above were placed in 0.35 mL of fresh serum-free RPMI medium 1640. Virus dilutions were prepared in 150 μL of the same medium supplemented with 40 μg/mL Polybrene (Sigma-Aldrich) and were added to the stromal cells. After 3 h of infection, the medium was further supplemented with 10% FCS. Following an additional 16 h of infection, the

medium was changed to 1 mL of fresh RPMI 1640 supplemented with 10% FCS, 1% penicillin/streptomycin, and 1% GlutaMAX (all from Gibco Life Technologies). Infection efficiency was assessed using fluorescence microscopy. After visual examination, stromal cells were trypsinized and mixed with crypts as previously described (24). To minimize the use of reagents and for increased convenience of analysis, we adjusted the coculture conditions to 96-well plates. Each well received 2,000 crypts mixed with 10,000 adenovirus-infected stromal cells resuspended in 30 μL of Matrigel.

RSPO Activity Assays with Reporter Cell Lines. STF3A cells (HEK293 cells with an integrated Super8XTOPflash reporter) were cultured and plated at a density of 50,000 cells per well in 24-well plates. STF3A cells were transfected 24 h post plating with total 600 ng of the indicated expression plasmids [2–200 ng Myc-tagged RSPO1 or RSPO3 (catalog nos. RC217921 and RC205016, respectively; OriGene), 200 ng pCS-mCherry as reference, 200–398 ng pPGK as empty vector, in Lipofectamine 2000 (catalog no. 11668019; Life Technology)]. Cells were harvested 16 h post transfection in PBS with 0.6% IGEPAL-CA630. Luciferase activity was measured as previously described (56). For recombinant RSPO1 and RSPO3 experiments, STF3A cells were cultured in DMEM with 10% FBS in 24-well plates, and the next day the medium was changed to 0.1% FBS with recombinant RSPO1 or RSPO3 protein (catalog nos. 7150-RS-025 and 4120-RS-025, respectively; R&D Systems) as indicated (100 pg/mL to 500 ng/mL). Luciferase activity was measured 16 h later and normalized to LDH activity.

Real-Time qPCR, Immunohistochemistry, and Fluorescence Visualization. Real-time qPCR was performed as previously described (24). qPCR primers are listed in Table S1. To image organoid–stromal interactions, stroma from *Rosa^mTmG^* mice was purified, cultured, and mixed with intestinal crypts derived from gender-matched *Lgr5-IRES-CreER^T2^-EGFP* mice and cultured in medium with no externally added R-spondins for 5 d. Thereafter, growth medium was pulsed with 2.5 μM Hoechst 33343, and organoids were imaged as soon as nuclei were labeled (typically within 10–15 min) using a Zeiss LSM 710 confocal microscope. Immunohistochemistry was performed as outlined in *Supporting Information*. An Operetta high-content screening system (PerkinElmer) was used to image stromal cell cultures. Image analysis and quantification procedures were performed using Columbus software (PerkinElmer).

DSS-Induced Colitis. DSS (TdB Consultancy) was dissolved at 2.5% in auto-claved tap water and provided ad libitum as drinking water to mice for a period of 5 d. The mice were killed at day 5, and their intestines were fixed in 4% buffered formalin and subjected to histochemical analysis as described previously (24).

Statistical Analysis. Data were analyzed using nonparametric statistical tests where applicable using Prism 5 software and R 3.2.1. The estimation of EC$_{50}$ was performed in R 3.2.1, using the drc software package (57).

1. Clevers H (2013) The intestinal crypt, a prototype stem cell compartment. *Cell* 154: 274–284.
2. Kuhnert F, et al. (2004) Essential requirement for Wnt signaling in proliferation of adult small intestine and colon revealed by adenoviral expression of Dickkopf-1. *Proc Natl Acad Sci USA* 101:266–271.
3. Korinek V, et al. (1998) Depletion of epithelial stem-cell compartments in the small intestine of mice lacking Tcf-4. *Nat Genet* 19:379–383.
4. Yan KS, et al. (2017) Non-equivalence of Wnt and R-spondin ligands during Lgr5+ intestinal stem-cell self-renewal. *Nature* 545:238–242.
5. Storm EE, et al. (2016) Targeting PTPRK-RSPO3 colon tumours promotes differentiation and loss of stem-cell function. *Nature* 529:97–100.
6. Sato T, et al. (2009) Single Lgr5 stem cells build crypt-villus structures in vitro without a mesenchymal niche. *Nature* 459:262–265.
7. Ootani A, et al. (2009) Sustained in vitro intestinal epithelial culture within a Wnt-dependent stem cell niche. *Nat Med* 15:701–706.
8. Kazanskaya O, et al. (2004) R-spondin2 is a secreted activator of Wnt/beta-catenin signaling and is required for Xenopus myogenesis. *Dev Cell* 7:525–534.

9. Moad HE, Pioszak AA (2013) Reconstitution of R-spondin:LGR4:ZNRF3 adult stem cell growth factor signaling complexes with recombinant proteins produced in Escherichia coli. *Biochemistry* 52:7295–7304.
10. Gong X, et al. (2012) LGR6 is a high affinity receptor of R-spondins and potentially functions as a tumor suppressor. *PLoS One* 7:e37137.
11. Warner ML, Bell T, Pioszak AA (2015) Engineering high-potency R-spondin adult stem cell growth factors. *Mol Pharmacol* 87:410–420.
12. Ohkawara B, Glinka A, Niehrs C (2011) Rspo3 binds syndecan 4 and induces Wnt/PCP signaling via clathrin-mediated endocytosis to promote morphogenesis. *Dev Cell* 20: 303–314.
13. de Lau WBM, Snel B, Clevers HC (2012) The R-spondin protein family. *Genome Biol* 13:242.
14. Xie Y, et al. (2013) Interaction with both ZNRF3 and LGR4 is required for the signalling activity of R-spondin. *EMBO Rep* 14:1120–1126.
15. Binnerts ME, et al. (2007) R-spondin1 regulates Wnt signaling by inhibiting internalization of LRP6. *Proc Natl Acad Sci USA* 104:14700–14705.
16. Hao H-X, et al. (2012) ZNRF3 promotes Wnt receptor turnover in an R-spondin-sensitive manner. *Nature* 485:195–200.

17. de Lau W, Peng WC, Gros P, Clevers H (2014) The R-spondin/Lgr5/Rnf43 module: Regulator of Wnt signal strength. *Genes Dev* 28:305–316.

18. Seshagiri S, et al. (2012) Recurrent R-spondin fusions in colon cancer. *Nature* 488:660–664.

19. Robinson D, et al. (2015) Integrative clinical genomics of advanced prostate cancer. *Cell* 161:1215–1228.

20. Watson AL, et al. (2013) Canonical Wnt/β-catenin signaling drives human schwann cell transformation, progression, and tumor maintenance. *Cancer Discov* 3:674–689.

21. Chartier C, et al. (2016) Therapeutic targeting of tumor-derived R-spondin attenuates β-catenin signaling and tumorigenesis in multiple cancer types. *Cancer Res* 76:713–723.

22. Kim K-A, et al. (2005) Mitogenic influence of human R-spondin1 on the intestinal epithelium. *Science* 309:1256–1259.

23. Kang E, Yousefi M, Gruenheid S (2016) R-spondins are expressed by the intestinal stroma and are differentially regulated during Citrobacter rodentium- and DSS-induced colitis in mice. *PLoS One* 11:e0152859.

24. Kabiri Z, et al. (2014) Stroma provides an intestinal stem cell niche in the absence of epithelial Wnts. *Development* 141:2206–2215.

25. Coombs GS, et al. (2010) WLS-dependent secretion of WNT3A requires Ser209 acylation and vacuolar acidification. *J Cell Sci* 123:3357–3367.

26. Adegboyega PA, Mifflin RC, DiMari JF, Saada JI, Powell DW (2002) Immunohistochemical study of myofibroblasts in normal colonic mucosa, hyperplastic polyps, and adenomatous colorectal polyps. *Arch Pathol Lab Med* 126:829–836.

27. Artells R, Navarro A, Diaz T, Monzó M (2011) Ultrastructural and immunohistochemical analysis of intestinal myofibroblasts during the early organogenesis of the human small intestine. *Anat Rec (Hoboken)* 294:462–471.

28. Mifflin RC, Pinchuk IV, Saada JI, Powell DW (2011) Intestinal myofibroblasts: Targets for stem cell therapy. *Am J Physiol Gastrointest Liver Physiol* 300:G684–G696.

29. Neufeld S, et al. (2012) A conditional allele of Rspo3 reveals redundant function of R-spondins during mouse limb development. *Genesis* 50:741–749.

30. Karlsson L, Lindahl P, Heath JK, Betsholtz C (2000) Abnormal gastrointestinal development in PDGF-A and PDGFR-(alpha) deficient mice implicates a novel mesenchymal structure with putative instructive properties in villus morphogenesis. *Development* 127:3457–3466.

31. Vannucchi MG, Traini C, Manetti M, Ibba-Manneschi L, Faussone-Pellegrini MS (2013) Telocytes express PDGFRα in the human gastrointestinal tract. *J Cell Mol Med* 17:1099–1108.

32. Roesch K, et al. (2008) The transcriptome of retinal Müller glial cells. *J Comp Neurol* 509:225–238.

33. Muzumdar MD, Tasic B, Miyamichi K, Li L, Luo L (2007) A global double-fluorescent Cre reporter mouse. *Genesis* 45:593–605.

34. Pinto D, Gregorieff A, Begthel H, Clevers H (2003) Canonical Wnt signals are essential for homeostasis of the intestinal epithelium. *Genes Dev* 17:1709–1713.

35. Itzkovitz S, Blat IC, Jacks T, Clevers H, van Oudenaarden A (2012) Optimality in the development of intestinal crypts. *Cell* 148:608–619.

36. Al-Nafussi AI, Wright NA (1982) Cell kinetics in the mouse small intestine during immediate postnatal life. *Virchows Arch B Cell Pathol Incl Mol Pathol* 40:51–62.

37. Ferrer-Vaquer A, et al. (2010) A sensitive and bright single-cell resolution live imaging reporter of Wnt/ß-catenin signaling in the mouse. *BMC Dev Biol* 10:121.

38. van Es JH, et al. (2005) Wnt signalling induces maturation of Paneth cells in intestinal crypts. *Nat Cell Biol* 7:381–386.

39. Aoki R, et al. (2016) Foxl1-expressing mesenchymal cells constitute the intestinal stem cell niche. *Cell Mol Gastroenterol Hepatol* 2:175–188.

40. Stzepourginski I, et al. (2017) CD34+ mesenchymal cells are a major component of the intestinal stem cells niche at homeostasis and after injury. *Proc Natl Acad Sci USA* 114:E506–E513.

41. Song S, Ewald AJ, Stallcup W, Werb Z, Bergers G (2005) PDGFRbeta+ perivascular progenitor cells in tumours regulate pericyte differentiation and vascular survival. *Nat Cell Biol* 7:870–879.

42. Festa E, et al. (2011) Adipocyte lineage cells contribute to the skin stem cell niche to drive hair cycling. *Cell* 146:761–771.

43. Hoch RV, Soriano P (2003) Roles of PDGF in animal development. *Development* 130:4769–4784.

44. Kurahashi M, et al. (2013) A novel population of subepithelial platelet-derived growth factor receptor α-positive cells in the mouse and human colon. *Am J Physiol Gastrointest Liver Physiol* 304:G823–G834.

45. Cretoiu D, Radu BM, Banciu A, Banciu DD, Cretoiu SM (2017) Telocytes heterogeneity: From cellular morphology to functional evidence. *Semin Cell Dev Biol* 64:26–39.

46. Stanganello E, et al. (2015) Filopodia-based Wnt transport during vertebrate tissue patterning. *Nat Commun* 6:5846.

47. Miyoshi H, Stappenbeck TS (2013) In vitro expansion and genetic modification of gastrointestinal stem cells in spheroid culture. *Nat Protoc* 8:2471–2482.

48. Durand A, et al. (2012) Functional intestinal stem cells after Paneth cell ablation induced by the loss of transcription factor Math1 (Atoh1). *Proc Natl Acad Sci USA* 109:8965–8970.

49. Kim TH, Escudero S, Shivdasani RA (2012) Intact function of Lgr5 receptor-expressing intestinal stem cells in the absence of Paneth cells. *Proc Natl Acad Sci USA* 109:3932–3937.

50. Farin HF, Van Es JH, Clevers H (2012) Redundant sources of Wnt regulate intestinal stem cells and promote formation of Paneth cells. *Gastroenterology* 143:1518–1529.e7.

51. San Roman AK, Jayewickreme CD, Murtaugh LC, Shivdasani RA (2014) Wnt secretion from epithelial cells and subepithelial myofibroblasts is not required in the mouse intestinal stem cell niche in vivo. *Stem Cell Reports* 2:127–134.

52. Kabiri Z, et al. (2015) Wnts are dispensable for differentiation and self-renewal of adult murine hematopoietic stem cells. *Blood* 126:1086–1094.

53. Liu S, et al. (2013) Lgr4 gene deficiency increases susceptibility and severity of dextran sodium sulfate-induced inflammatory bowel disease in mice. *J Biol Chem* 288:8794–8803, discussion 8804.

54. Biechele S, Cockburn K, Lanner F, Cox BJ, Rossant J (2013) Porcn-dependent Wnt signaling is not required prior to mouse gastrulation. *Development* 140:2961–2971.

55. Barker N, et al. (2007) Identification of stem cells in small intestine and colon by marker gene Lgr5. *Nature* 449:1003–1007.

56. Proffitt KD, Virshup DM (2012) Precise regulation of porcupine activity is required for physiological Wnt signaling. *J Biol Chem* 287:34167–34178.

57. Ritz C, Baty F, Streibig JC, Gerhard D (2015) Dose-response analysis using R. *PLoS One* 10:e0146021.

DEVELOPMENTAL BIOLOGY